Durability enhancements in concrete with fiber reinforcement

N. Banthia
The University of British Columbia, Vancouver, Canada

ABSTRACT: Lack of durability in concrete structures remains one of the pressing challenges of our time. By one estimate, most structures built today will require some kind of repair intervention within the first eighteen years of their lives. This paper argues that fiber reinforcement is one of the most cost-effective means of enhancing the durability of concrete. In this context, two reinforcement mechanisms are discussed: first, crack suppression in the early stages of hydration when high shrinkage strains occur, and second, in-service when mitigation in the transport properties occurs under an applied stress. The paper proposes a Service Life Predictions Model which indicates that at least in qualitative terms, fiber reinforced concrete will depict a better durability in service than plain concrete.

1 INTRODUCTION

Cracking in concrete remains a paramount concern for both structural safety and long term durability. Cracking will reduce the load carrying capacity of a structural component, but more importantly, cracking enhances the permeability and penetrability of concrete to deleterious agents (water, chloride, sulphates, etc.) and accelerates deterioration due to scaling, freeze-thaw, alkali-silica reactivity, sulphate attack and rebar corrosion. Cracking can be induced in concrete by plastic shrinkage, drying shrinkage, service loads, accidental impact, fatigue, and geotechnical incompatibility.

Fiber reinforcement is now considered as the most effective way of improving the resistance of concrete to cracking. During the last two decades, numerous fiber types made from many different materials (steel, polypropylene, nylon, carbon, etc.) have been developed and successfully used to reinforce concrete. While the primary purpose of fiber reinforcement has so far been to improve the toughness and energy absorption of concrete, it is becoming apparent that the real benefit of fiber reinforcement may in fact be in improving the physical and durability properties of concrete.

The purpose of this paper is to understand the role of fiber reinforcement in concrete at two stages of its life. At early ages, when concrete undergoes large volumetric deformations due to plastic shrinkage and later on when concrete is in service and subjected to live loads. For the first, results of plastic shrinkage cracking tests are described, and for the second, data from permeability tests under stress are given. The results from the latter are then applied to a Service Life Predictions Model which indicates that, at least in qualitative terms, fiber reinforced concrete will depict a better durability in service than plain concrete.

2 ROLE OF FIBER REINFORCEMENT AT EARLY AGES: CONTROL OF SHRINKAGE CRACKING

When concrete is in the plastic state, moisture loss may occur both by evaporation to the atmosphere and absorption by subbase or formwork. Although some of the water lost this way is replenished by bleeding, if the surface moisture loss exceeds 0.5 $kg/m^2/h$ [Mindess et al. 2003], negative capillary pressures develop in concrete causing internal compressive strains. If concrete is restrained, these compressive strains may result in tensile stresses far in excess of those needed to cause cracking in young concrete with poorly developed strength. The most effective technique of mitigating plastic shrinkage cracking is by preventing the loss of water from the concrete surface by extended curing. In some instances, however, curing alone is not adequate, and additional measures need to be adopted. These include temperature control, shielding from high
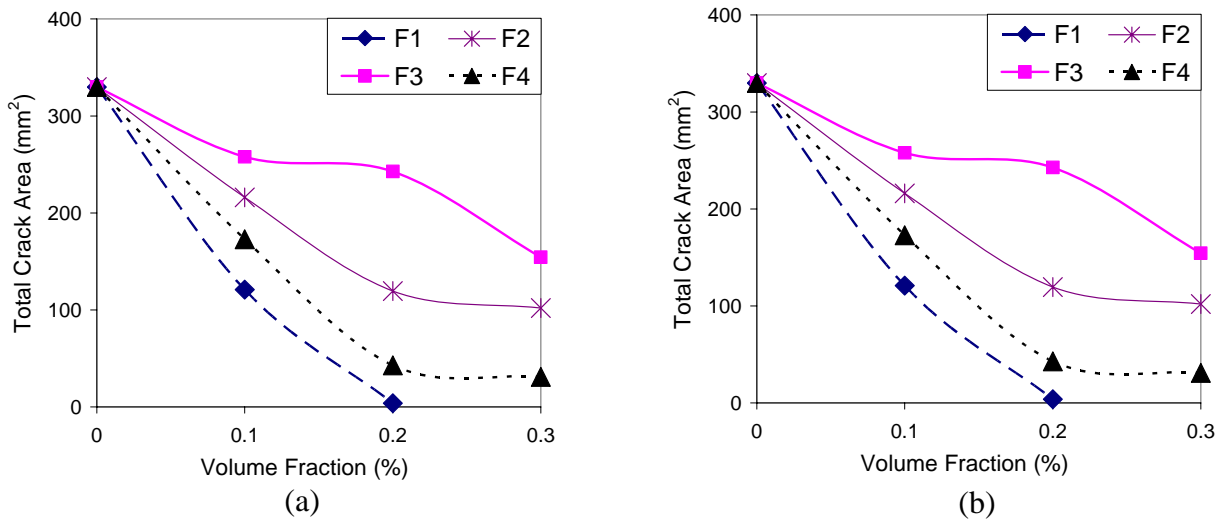
Figure 1. (a) Total Crack Area and (b) Maximum Crack Width for Various Fiber Types F1: Mono-filament 3d - 1/2"; F2: Monofilament 6d - 1/2"; F3: Monofilament 6d - 1/4"; F4: Fibrillated 1000d - 1/2"
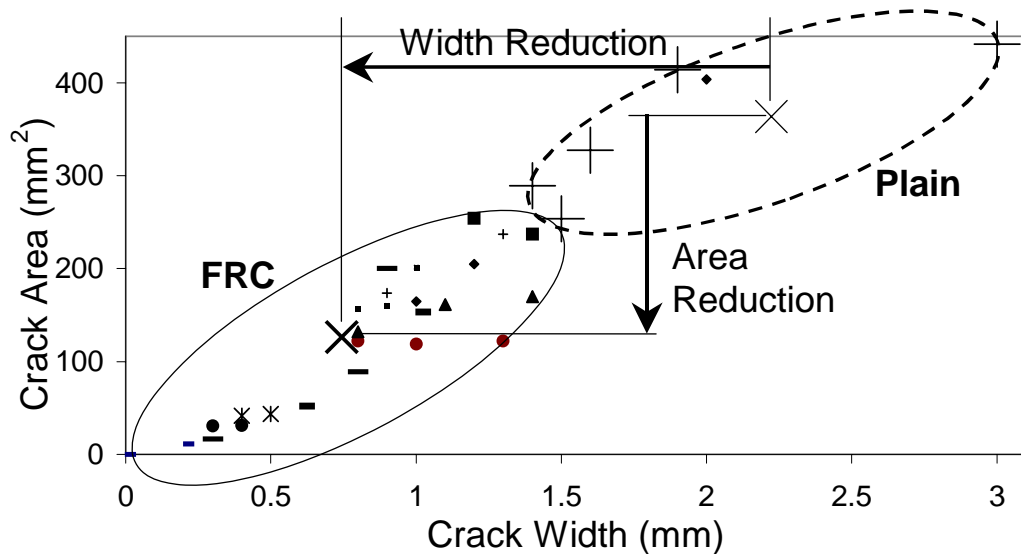

Figure 2. Comparison between Plain and Fiber Reinforced Concrete based on Crack Area and Crack Widths. Notice a reduction in both crack area and crack width due to fiber reinforcement.
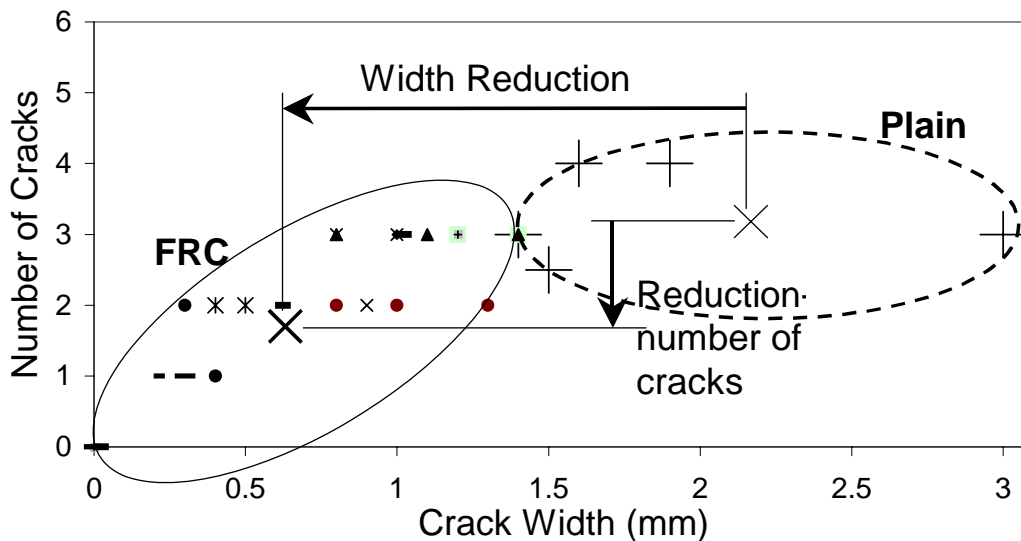

Figure 3. Comparison between Plain and Fiber Reinforced Concrete based on Crack Width and Number of Cracks. Notice a reduction in both the crack width and number of cracks due to fiber reinforcement.

winds, reduced use of admixtures that prevent bleeding and the use of shrinkage reducing admixtures [Weiss & Shah 1997, Shah et al. 1992]. One highly effective technique of controlling plastic shrinkage cracking is by reinforcing concrete with fibers [Grzybowski & Shah 1990, Qi, Weiss, & Olek 1993]. This has been demonstrated by using a test procedure recently developed at the University of British Columbia [Banthia et al. 1996, Banthia & Yan 2000, Banthia & Gupta 2006a,b, Banthia et al. 2006]. In this method, a layer of fresh fiber reinforced concrete is placed as an overlay directly on a fully hardened substrate base. This 'substrate base' has protuberances, which enhances its roughness and, in turn, imposes a uniform restraint on the overlay. The whole assembly is then subjected to a drying environment to induce cracking in the overlay, which is then characterized using a high magnification microscope.

General influence of fiber reinforcement on crack pattern is shown in Figure 1 [Banthia & Gupta 2006a] where fibers are compared based on the total crack area and the maximum crack width. Notice the effectiveness of fibers in reducing cracking and a greater effectiveness at higher dosage rates. Fibrillated fibers can be seen to be more effective than the mono-filament fibers. In Figure 2, the crack areas noted in various individual tests are plotted against the maximum crack widths observed in these tests and in Figure 3, the number of cracks observed in individual tests is plotted against the maximum crack width. Centroids of the families of data points for plain overlays and fiber reinforced overlays are located in both these figures. Notice that the effect of fiber reinforcement is apparent in terms of reductions in crack area, maximum crack width and the number of cracks.

3 ROLE OF FIBER REINFORCEMENT AT MATURE AGES: CONTROL OF TRANSPORT PROPERTIES

Penetration of deleterious substances into concrete via the two prominent modes of transport—permeation and diffusion—remains the single most important factor controlling the rate of concrete degradation [Sanjuan & Munoz-Martialay 1997, Basheer et al. 2001]. Permeability of concrete, in turn, is influenced by two primary factors [Mehta, & Monteiro 1993]: interconnected porosity in the cement paste and micro-cracks in the concrete. Porosity in the cement paste and the extent of its interconnectivity are controlled for most part by the w/c ratio, degree of hydration, and the degree of compaction. Density and location of interfacial micro-cracks, on the other hand, are determined by the level of applied stress or deformation, external or internal, experienced by the concrete. Internal stresses and deformation occur in concrete as a result of shrinkage, thermal gradients, abrupt changes in the hygro-thermal environment and factors causing volumetric instability. External stresses and deformations arise as a result of imposed dead and live loads. Depending on the boundary conditions, capillary suction, if it occurs, will act as a precursor to saturation and aid some of the mechanisms cited above.

Diffusion of chlorides and other ions into the concrete depends primarily upon their concentration gradient. Even here, permeability plays a critical role in that a continuous fluid flow is necessary for the process of diffusion to continue; in the case of insufficient moisture, flow paths become interrupted and the diffusion process would cease [Kropp & Hilsdorf 1992]. Clearly, the transport of aggressive media into concrete is a complex process and no one single mechanism can fully describe or predict the onset or the rate of degradation. In research, however, an attempt is often made to limit the flow of media to one single transport mechanism so that transport coefficients can be derived according to some acceptable model of that specific transport process. While it is unfortunately not always easy to predict one transport coefficient from another, water permeability is often considered to be an excellent parameter to assess the vulnerability of concrete to deterioration. In the text to follow, results of permeability tests carried out on plain and fiber reinforced concrete with and without an applied stress are described [Banthia & Bhargava 2007].

A schematic representation of the apparatus designed for carrying out water permeability tests on concrete in the presence of an applied stress is shown in Figure 4. The apparatus is described in detail elsewhere [Bhargava et al. 2006]. In brief, water is allowed to permeate through a cylindrical concrete specimen 102 mm diameter and 204 mm long with a 50 mm diameter hollow cylindrical core and the mass of water thus permeated under equilibrium conditions is collected. The permeability cell is mounted in a 200 kN hydraulic Universal Testing Machine (UTM) such that a uniform compressive stress can be applied directly on the concrete specimen housed in the cell. The water collected is related to the coefficient of water permeability (K_w) by applying Darcy's law:
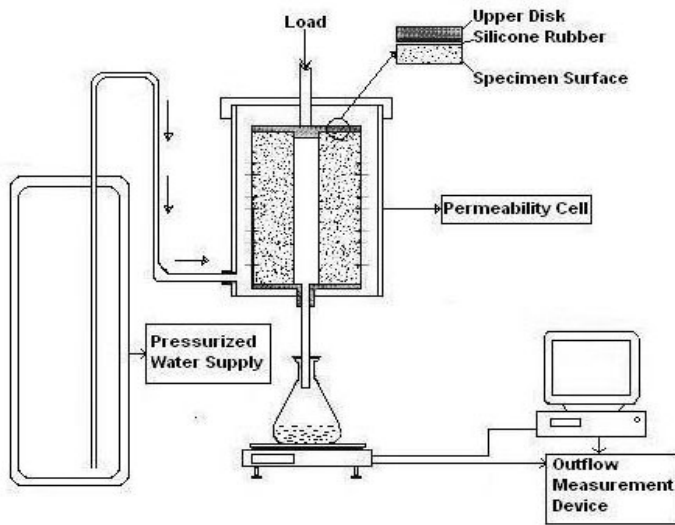
Figure 4. Setup for Water Permeability Tests

$$K_w = \frac{QL}{A\Delta h} \tag{1}$$

K_w = Coefficient of water permeability (m/s), Q = Rate of Water Flow (m³/s), L = Thickness of specimen wall (m), A = Permeation area (m²) and Δh = Pressure head (m)

In all tests, pairs of specimens were tested, one under stress in the UTM and the other without any stress placed outside the UTM. All tests were conducted using a constant inflow water pressure of 0.48 MPa. Typically it took about 30 hours after the start of the test to achieve conditions of full flow equilibrium. Data recorded only after equilibrium were used in permeability analysis.

Two Series of tests were performed as follows:
Series I: Permeability tests were carried out on unstressed fiber reinforced concrete specimen and on a companion unstressed plain concrete specimen. Fiber volume fractions of 0.1, 0.3 and 0.5% were used. Two replicates were tested for each fiber volume fraction. The fiber used was a virgin, fully purified, cellulose fiber with an average length of about 2.3 mm, collated and with a surface treatment to enhance their alkali tolerance and bond with concrete.
Series II: Permeability tests were carried on stressed specimens of plain and fiber reinforced concrete. Two applied stress levels of $0.3f_u$ and $0.5f_u$ were investigated, where f_u represents the strength of concrete in compression at the time of the test. As in Series I, fiber volume fractions of 0.1, 0.3 and 0.5%

were used. Each test under stress was performed with a companion specimen under no stress.

Representative Series I permeability data are given in Figure 5 where fiber reinforced concrete with 0.5% fiber by volume is compared with plain concrete. The plots for 0.1% and 0.3% look similar with somewhat reduced fiber effectiveness than 0.5%. Notice that fiber reinforcement was significantly effective in reducing the permeability of concrete. The permeability coefficients calculated over a 12 hour period were averaged to obtain an average value of permeability for the specimen. Due to the large variability normally associated with water permeability results, it is often advisable to compare permeability data based on ratios [Sanjuan & Munoz-Martialay 1997]. To quantify the effect of fiber reinforcement in unstressed conditions, ratios of the permeability R_I (I indicating Series I) between FRC and plain concrete were calculated using the following equation.

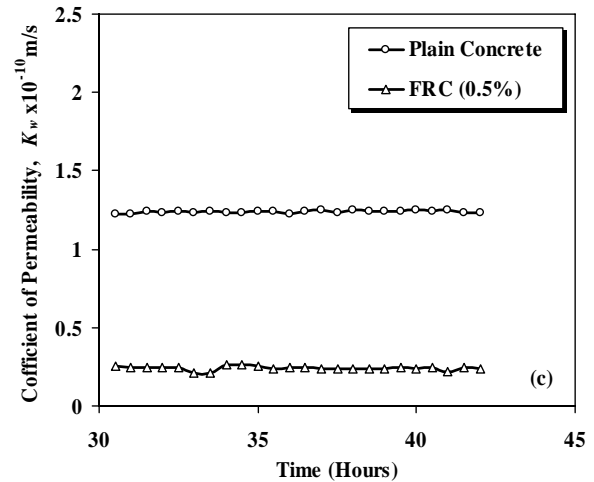$$R_I = \frac{K_{w_{FRC}}}{K_{w_{PC}}} \tag{2}$$

Figure 5. Permeability Plots for Plain and FRC with 0.5% Fiber Volume

where $K_{w_{FRC}}$ = average water permeability coefficient for fiber reinforced concrete without stress

$K_{w_{PC}}$ = average water permeability coefficient for plain concrete without stress

The values of calculated R_I are plotted in Figure 6. Notice that the average permeability of FRC with 0.1%, 0.3% and 0.5% fiber was, respectively, 0.57, 0.36 and 0.18 times that of plain concrete under conditions of no stress.

The reduction in the water permeability of unstressed concrete due to fiber reinforcement as seen in Figure 6 is in agreement with the results of Sanjuan et al., [Sanjuan et al.1991] but contrary to the findings of Al-Tayyib and Al-Zahrani [Al-Tayyib, A.J. & Al-Zahrani 1990]. A reduction in permeability due to fiber reinforcement can be related to the two known mechanisms. First, fibers produce mix stiffening, reduce the settlement of aggregates, and decrease bleeding. This, in turn, is expected to reduce the formation of bleed channels and decrease the ease with which flow can occur through the material [Zollo et al. 1986]. Secondly, hydrophilic fibers such as cellulose are expected to better engage water in the mix and reduce the overall early age shrinkage.

Based on results of Series II tests, representative permeability plots for plain concrete and FRC with 0.5% fiber reinforcement under various levels of applied stress are given in Figures 7a-b, respectively.
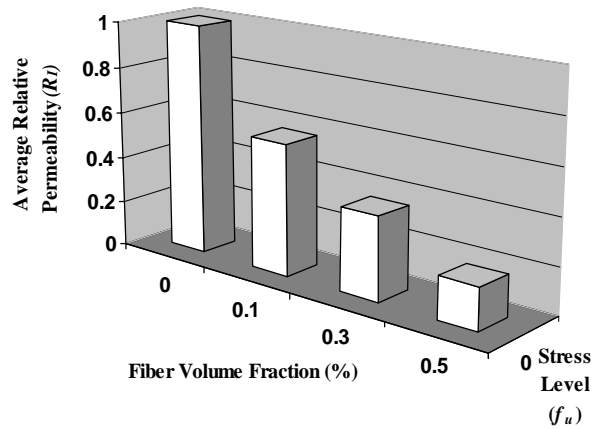
Fig. 6 Permeability without Stress (Series I)

The plots for 0.1% and 0.3% look similar with somewhat reduced fiber effectiveness than 0.5% and are not reproduced in the interest of brevity. Notice in Fig. 7a-b that the stress had a decisive influence on the permeability of both plain and fiber reinforced concrete.

Due to the large variability normally associated with water permeability results, in order to facilitate comparison, the permeability data were normalized and compared as ratios.
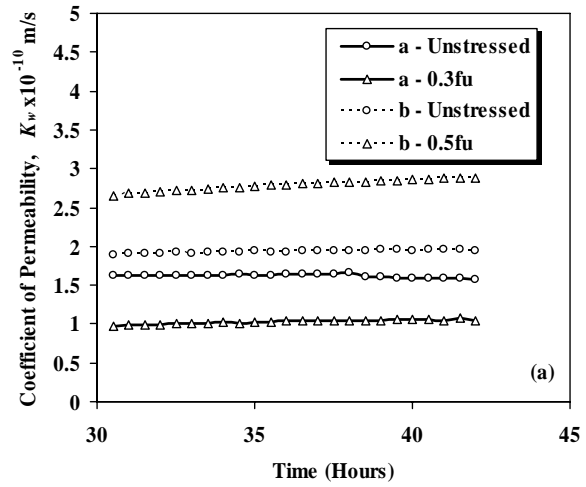
Figure 7a. Permeability Plots for Plain Concrete at Various Levels of Stress ('a' and 'b' represent two pairs of specimens where each pair was tested separately)
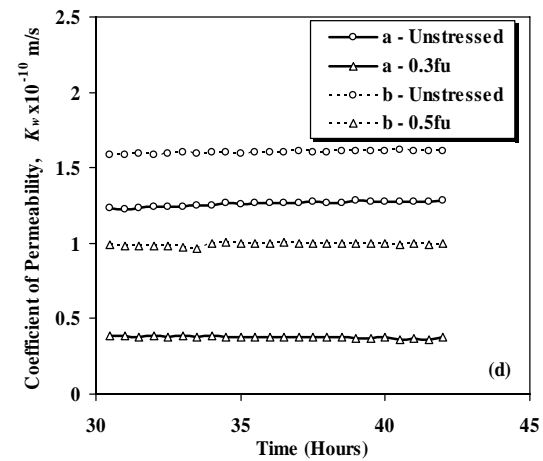
Figure 7b. Permeability Plots for FRC with 0.5% Fiber at Various Levels of Stress ('a' and 'b' represent two pairs of specimens where each pair was tested separately)

To quantify the effect of stress, ratios of the permeability R_{II} (II indicating Series II) for a specific material (plain or FRC) were calculated by using the following Equation:

$$R_{II} = \frac{K_{w_{stressed}}}{K_{w_{unstressed}}} \qquad (3)$$

where $K_{w_{stressed}}$ = average water permeability coefficient under stress

$K_{w_{unstressed}}$ = average water permeability coefficient without stress

The values of calculated R_{II} are plotted in Fig. 8. Notice that when the stress was first increased to $0.3f_u$, both plain and FRC showed a decrease in the permeability. However, when the stress was

increased to $0.5f_u$, plain and FRC showed very different trends. At $0.5f_u$, the permeability of plain concrete increased substantially over that of the unstressed specimen, but for FRC, while there was an increase in the permeability over $0.3f_u$, the permeability still stayed below that of the unstressed specimen.

In order to obtain a 'holistic' view of the above test results, i.e. to compare permeability values for plain and fiber reinforced concrete with and without stress using a common and reliable datum, 'normalized' permeability coefficients were calculated as follows:

The permeability of plain concrete under zero stress condition was chosen as the common reference point against which all other permeability coefficients were normalized. To obtain a high statistical confidence in this reference datum, ten replicates of plain concrete under no stress were analyzed to obtain the most statistically significant value of its permeability coefficient. The most statistically significant value of $K_{w\,plain-unstressed}$ was found to be 1.66×10^{-10} m/s. In order to compare the permeability coefficients obtained from other series with $K_{w\,plain-unstressed}$, an overall correlation constant $R_{I,\,II}$ was calculated as,

$$R_{I,\,II} = R_I \times R_{II} \qquad (4)$$

The 'normalized' permeability coefficients were then calculated by taking a product of the overall correlation constant $R_{I,\,II}$ and $K_{w\,plain-unstressed}$.

$$K_{normalized} = K_{w\,plain-unstressed} \times R_{I,\,II} \qquad (5)$$

The rationale for Eq. 5 is as follows: R_I (Eq. 2) expresses the influence of fibers in the unstressed state and R_{II} (Eq.3) expresses the influence of stress on permeability of a given materials (plain or FRC). Collectively, therefore, $R_{I,\,II}$ expresses the relationship between permeability of a given material (plain or FRC) and that of plain concrete under no stress. This calculation is based on the assumption that the average value of water permeability coefficient for FRC under zero stress condition should be the same for Series I and Series II experiments. The normalized permeability coefficients for plain and FRC under various stress levels are plotted in Figure 9.

The normalized permeability data indicate that stress has a significant influence on the permeability of concrete. An initial stress increase to $0.3f_u$ reduced the permeability of both plain and FRC. This can be directly attributed to pore compression that would occur under stress. However, at stresses greater than $0.3f_u$, while both plain and FRC show an increase in the permeability, the increases in plain concrete were significantly greater than that in the FRC. In the case of FRC, at $0.5f_u$, the permeability increased, but still stayed at a level below the unstressed level.
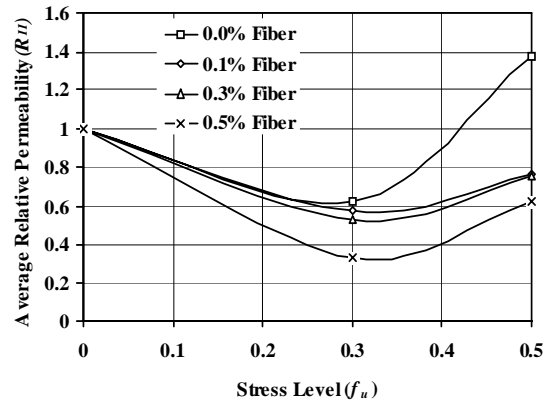

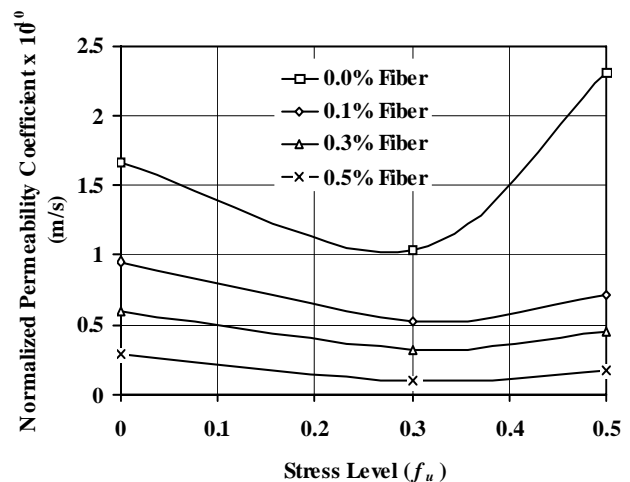Figure 8. Influence of Stress on Relative Permeability

Figure 9. Normalized Permeability Coefficients

4 SERVICE LIFE PREDICTION

Studies relating different transport coefficients are rare. In particular, experimental data relating permeability and diffusion coefficient is lacking, and only a theoretical correlation can be established between these two coefficients via a correlation constant. Such a correlation constant was determined in this study.

Empirical equations for the permeability coefficient were proposed by Hedegaard et al. [Hedegaard & Hansen 1992] and for diffusion coefficient were proposed by Hansen et al. [Hansen et al. 1986] as follows:

$$K_w = \exp\left[-4.3\left(\frac{c+0.31f}{w}\right)+4.0\right] \qquad (6)$$

$$D = 1.7x10^{-\left(\frac{c+0.3f}{w}+7.0\right)} \qquad (7)$$

$K_w=$ water permeability coefficient (m/s)
$D =$ chloride ion diffusion coefficient, in cm^2/s
$c =$ cement content of concrete, in kg/m^3
$w=$ water content of concrete, in kg/m^3
$f =$ fly-ash content of concrete, in kg/m^3

By Substituting the values of c, w and f for concrete being tested, one obtains $K_w=1.07x10^{-10}$ (m/s) and $D = 7.89x10^{-13}$ (m^2/s). Further, the permeability K (m^2) of a single straight pore with effective pore radius r_{eff} embedded in a medium of cross-sectional area A can be related to effective pore radius by assuming *Hagen-Poiseuille's* law to be valid for small pores.

$$K = \frac{\pi r_{eff}^4}{8A} \qquad (8)$$

where r_{eff} is the effective pore radius defined as the radius of the effective pores which take part in the transport. Also, the diffusion coefficient can be related to the area fraction of effective pores as,

$$D = D_o a_{eff} = D_o \frac{\pi r_{eff}^2}{A} \qquad (9)$$

where $a_{eff} =$ is the area fraction of effective pores

$D_o =$ is the diffusion coefficient in a bulk fluid

Assuming that the effective pore radius in Equations 8 and 9 is the same, a general relationship between permeability K (m^2) and diffusion coefficients D (m^2/s) emerges [Garboczi 1990],

$$K = \frac{r_{eff}^2}{8D_o}D \qquad (10)$$

Further, it is to be noted that an interconnected pore system is necessary for a continuous network of flow paths to be available for various transporting media. In saturated conditions, the steady state flow coefficient can be related to the water permeability coefficient as the two processes occur simultaneously,

$$K_w = \frac{K}{\eta / \rho g} \qquad (11)$$

Using Equations 10 and 11, the water permeability coefficient K_w (m/s) and the diffusion coefficient D (m^2/s) can be related as,

$$K_w = \frac{r_{eff}^2 \rho g}{8D_o \eta}D \qquad (12)$$

where K_w as before is the water permeability coefficient (m/s),
D is the diffusion coefficient (m^2/s),
r_{eff} is the effective pore radius,
η is the viscosity of water (Ns/m^2),
ρ is the density of water (kg/m^3) and,
g is the gravity (m/s^2)

This equation corresponds to Katz-Thompson Equation (9), and is based on the assumption that the effective radius affecting the permeability and the diffusion coefficient is same.

Equation 12 can be further modified to consider the effect of stress and the fibers on concrete. Since the permeability coefficient is proportional to the fourth power of effective pore radius (Eq. 8) and since the normalized permeability coefficient is related to the water permeability coefficient of unstressed plain concrete through the two previously defined factors F and S, the effective pore radius can be modified to consider the effect of fiber reinforcement and stress on concrete:

$$r_{normalized}^* = F^{0.25}S^{0.25}r_{eff} \qquad (13)$$

where, $r^*_{normalized}$ is the effective pore radius corresponding to normalized permeability values and r_{eff} in this case is the effective pore radius of plain concrete under zero stress condition.
Substituting Eq.13 into Eq.12, we get a modified equation which relates normalized water permeability to diffusion coefficient as,

$$K_{normalized} = CF^{0.5}S^{0.5}D \qquad (14)$$

where $C = \frac{r_{eff}^2 \rho g}{8D_o \eta}$ is a constant proportional to second power of the effective pore radius of plain concrete under zero stress condition.

For plain concrete and zero stress condition $F=S=1$ and for this case:

$$K_{normalized} = K_{w\,plain-unstressed} = CxD \qquad (15)$$

Substituting the empirical values of the water permeability coefficient $K_w=1.07\times10^{-10}$ m/s and the chloride ion diffusion coefficient $D = 7.89\times10^{-13}$ m^2/s, as obtained previously, the value of constant C for the concrete in question can be calculated:

$$C = 135.62 \ \text{m}^{-1} \qquad (16)$$

The constant C computed above takes into consideration the effective pore radius of plain concrete under zero stress condition and properties of the chloride ion diffusion coefficient. The calculated chloride ion diffusion coefficients are given in Table 1.

Table 1. Computed Values of Chloride ion Diffusion Coefficient.

Fiber Volume Fraction V_f	Applied Stress Level	Normalized water permeability coefficient $K_{normalized}$x10^{-10} (m/s)	Chloride ion diffusion coefficient Dx10^{-13} (m^2/s)
0.0%	0.0f_u	1.66	12.24
	0.3f_u	1.03	9.64
	0.5f_u	2.30	14.43
0.1%	0.0f_u	0.95	9.27
	0.3f_u	0.53	6.85
	0.5f_u	0.71	7.95
0.3%	0.0f_u	0.60	7.37
	0.3f_u	0.32	5.40
	0.5f_u	0.45	6.38
0.5%	0.0f_u	0.30	5.21
	0.3f_u	0.10	3.02
	0.5f_u	0.18	3.97

In order to quantify the benefits of fiber reinforcement, Durability Factor, D, for a given concrete under a given stress level was defined as the ratio of its expected service life to that of companion plain concrete under zero stress.

There are two basic mechanisms which give rise to the corrosion of reinforcing steel in concrete: carbonation of concrete around the reinforcing bar and access of the chloride ions to the surface of the reinforcing bar. Here, only the second mechanism of corrosion was considered; i.e., corrosion would initiate when the concentration of chloride ions in concrete at the surface of reinforcing bars would exceed a certain threshold value. At such a threshold level, the passive layer that protects the reinforcing bars from corrosion is expected to be broken down and the corrosion is expected to initiate. In order to predict the length of the initiation period [Clifton et al. 1990] as determined by the depth of cover and the diffusion coefficient of concrete, the model developed by Tuutti's [Tuutti 1982] was employed. As per Tuutti's model (Figure 10), the service life (t) is expressed as the sum of the initiation (t_i) and propagation (t_p) period up to the threshold at which deterioration becomes unacceptable: $t=t_i+t_p$. However, in chloride induced corrosion, the service life is usually assumed to be equal to the initiation time i.e. $t=t_i$. This is because the initiation period is much longer than the propagation period and there is general uncertainty with the regards to the propagation period. Hence a conservative estimate is usually made by only considering the initiation period as was done in this study.
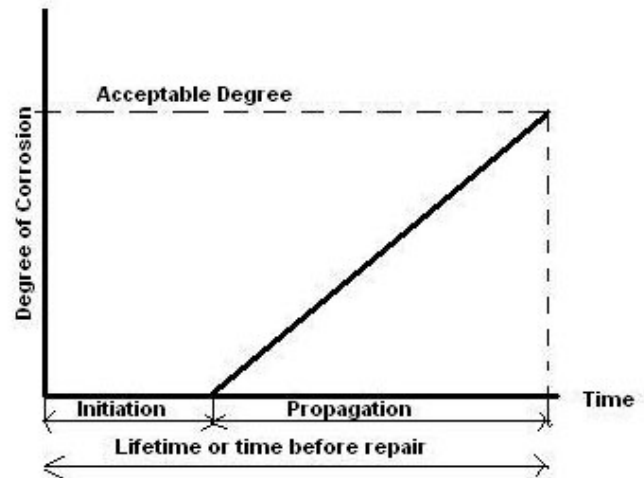

Figure 10. - Conceptual Model of Corrosion Initiation and Propagation after Tuutti [24]

In Tuutti's model, ingress of chlorides is estimated by a one-dimensional diffusion process using the Fick's Second Law of diffusion. For non-steady state condition, the chloride concentration C at a location x and at a time t is given by [Crank 1956].

$$\frac{\delta C}{\delta t} = \frac{\delta}{\delta x}\left(D \frac{\delta C}{\delta x} \right) \qquad (17)$$

Here, the diffusion coefficient D may be a constant or a function of other variables such as chloride concentration, location, time, temperature, etc. For a simple case with known geometry and boundary conditions where the diffusion coefficient D can be

assumed to be a constant, solution to Eq.17 is given by [Newman1970].

$$C(x,t) = C_s \left[1 - erf\left(\frac{x}{2\sqrt{Dt}} \right) \right] \qquad (18)$$

$$erf(z) = \frac{2}{\sqrt{\pi}} \int_0^z e^{-t^2} dt \qquad (19)$$

where,
erf is a standard error function,
x is effective concrete cover depth,
C_s is the concentration of the chloride ions at the outside surface of the concrete and is assumed to be constant with time. That is, $C = C_s$ for $x = 0$ and for any *t*
C_i is the concentration at the depth of the reinforcement; assumed to be zero at t =0.
C_t is the threshold concentration required to initiate steel reinforcement corrosion. The initiation period is accomplished when $C_i = C_t$ and,
t = time
Eq.18 can be solved by a using a normal standard distribution [Bertolini et al. 2004]:

$$erf(z) = 2N(z\sqrt{2}) - 1 \qquad (20)$$

$$N(z\sqrt{2}) = \frac{1}{\sqrt{2\pi}} \int_{-\infty}^{z\sqrt{2}} e^{\frac{t^2}{2}} dt \qquad (21)$$

The initiation time can thus be calculated by

assuming a constant diffusion coefficient for concrete, a known surface chloride content (dictated by the environment), the thickness of the concrete cover and critical chloride ion content at which onset of corrosion is expected.

Solving the above equation for C_t = threshold concentration of chloride ions = 0.50 % (based on the mass of cement), C_s =chloride ions concentration at the surface of concrete = 0.70 % (based on the mass of cement), $x = 25$ mm, and diffusion coefficients, *D,* from Table 1:

$$t \approx t_i = \frac{x^2}{0.2678D} \qquad (22)$$

Notice that a lower value of 0.50% threshold concentration of chloride ions was chosen due to the fact that fly ash was used in the concrete and is known to increase the rate of corrosion [Thomas 1996, Arya & Xu 1995]. The above equation predicts that service life of any concrete is proportional to x^2, and holds an inverse relationship with the chloride ion diffusion coefficient. Therefore doubling the concrete cover increases service life of concrete by a factor of 4, whereas a 10-fold reduction in diffusion coefficient will result in a 10-fold increase in the predicted service life. Substituting the values of diffusion coefficient from Table 1 into Eq. 22 for different concrete types and stress conditions, the Durability Factors were computed and plotted in Figure. 11.
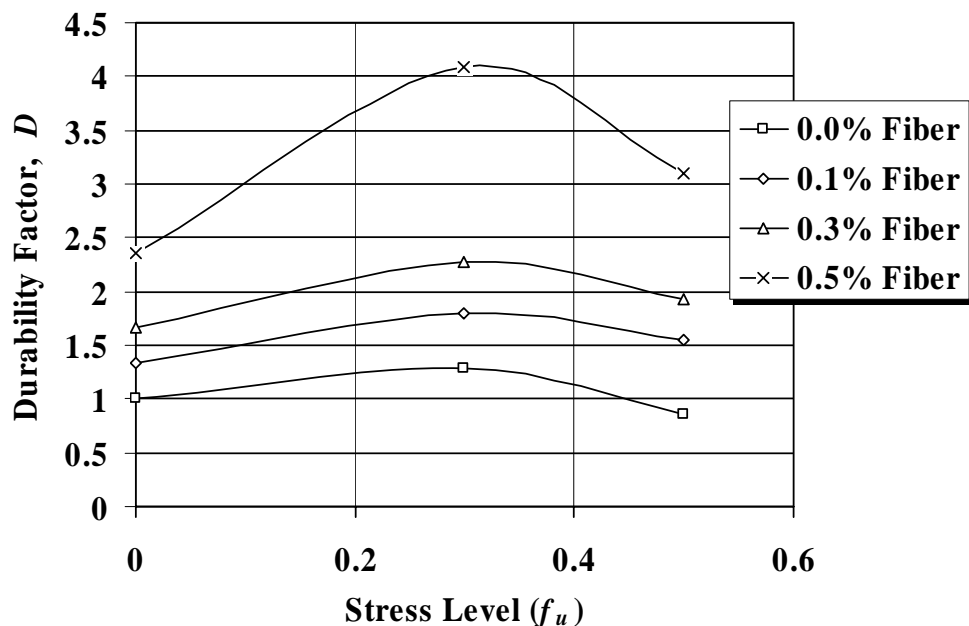

Figure 11. - Influence of Stress and fiber volume fraction on Durability factor D

5 CONCLUSIONS

The paper demonstrated that fiber reinforcement can help enhance the durability of concrete in two ways. First, it can reduce shrinkage cracking in early ages, and second, it can reduce the permeability of concrete in service under stress. When such findings are combined and applied to a Service Life Predictions Model (SLPM), there emerges a clear indication that structures built with concrete carrying even small dosages of fiber reinforcement may demonstrate large improvements in long term durability and service life performance.

REFERENCES

Al-Tayyib, A.J. & Al-Zahrani, M.M. 1990. *ACI Materials Journal*, 87(2): 108-113

Arya, C. & Xu, Y. 1995. Effect of cement type on chloride binding and corrosion of steel in concrete, *Cement and Concrete Research*, 25(4): 893-902.

Banthia, N., Yan, C. & Mindess, S. 1996. Restrained Shrinkage Cracking in Fiber Reinforced Concrete: A Novel Test Technique, *Cement and Concrete Research*, 26(1): 9-14.

Banthia, N. & Yan, C. 2000. Shrinkage Cracking in Polyolefin Fiber Reinforced Concrete, *American Concrete Institute, Materials Journal*, 97(4): 432-437.

Banthia, N. & Gupta, R. 2006a. Repairing with Fiber Reinforced Concrete Repairs, *ACI Concrete International*, 28(11) Nov. 2006: 36-40.

Banthia, N. & Gupta, R. 2006b. Influence of Polypropylene Fiber Geometry on Plastic Shrinkage Cracking in Concrete, Cement and Concrete Research, 36 (7) July 2006: 1263-1267.

Banthia, N., Gupta, R. & Mindess, S. 2006. Development of Fiber Reinforced Concrete Repair Materials, *Canadian J. of Civil Engineering*, 33(2) February 2006: 126-133.

Banthia, N. & Bhargava, A. 2007. Permeability of Stressed Concrete and Role of Fiber Reinforcement, *American Concrete Institute, Materials Journal*, 104(1) Jan-Feb 2007: 303-309.

Basheer, L., Kropp, J. & Cleland, D.J. 2001. Assessment of the Durability of Concrete from its Permeation Properties: A review, *Construction and Building Materials*, 15: 93-103.

Bertolini, L., Elsener, B., Pedeferri, P. & Polder, R. 2004. Corrosion of Steel in Concrete Prevention, Diagnosis, Repair, WILEY-VCH Verlag GmbH and Co. kGaA, Weinheim.

Bhargava, A., Banthia, N., and Biparva, A. 2006. An Experimental Technique for Measurement of Water Permeability of Stressed Concrete, Experimental Techniques, 30 (5), September-October 2006: 28-31

Clifton, J.R., Knab, L.I., Garboczi, E.J., & Xiong, L.X. 1990. Chloride Ion Diffusion in Low Water -to- Solid Cement Pastes," NISTIR 4549, National Institute of Standards and Technology, Gaithersburg, Md., Apr.

Crank J. 1956. Mathematics of diffusion, Oxford: Clarendon Press.

Garboczi, J. 1990. Permeability, diffusivity and microstructural parameters: A critical review, *Cement and Concrete Research*, 20(4): 590-601.

Grzybowski, M. & Shah, S.P. 1990. Shrinkage Cracking of Fiber Reinforced Concrete, *ACI Materials Journal*, March-April 1990: 138-148.

Hansen, T.C., Jensen, J. & Johannesson, T. 1986. Chloride Diffusion and Corrosion initiation of steel reinforcement in fly-ash concretes, *Cement and Concrete Research*, 16(5): 782-784.

Hedegaard, S.E., Hansen, T.C. 1992. Water permeability of fly ash concretes, *Materials and Structures*, 25: 381-387.

Kropp, J. & Hilsdorf, H.K. 1992. Performance Criteria for Concrete Durability, RILEM Report 9.

Mehta, P.K. & Monteiro, P J M. 1993. Concrete Structure, Properties, and Materials, Prentice Hall, Second Edition, New Jersey.

Mindess, S., Young, J. Francis & Darwin, D. 2003. Concrete, 2nd Edition, Prentice Hall, NJ.

Newman, A.B. 1970. The Drying of Porous Solids. Diffusion Calculations, *American Institute of Chemical Engineers*, V27.

Qi, C., Weiss, J. & Olek, J. 2003. Characterization of plastic shrinkage cracking in fiber reinforced concrete using image analysis and a modified Weibull function, *Materials and Structures*, 36(260) July 2003: 386-395.

Sanjuan, M.A. & Munoz-Martialay. 1997. M.A., Variability of the Concrete Air Permeability Coefficient with Time, *Building and Environment*, 32(1): 51-55.

Sanjuan, M.A. et al. 1991. *Proceedings Materials Research Society*, 211: 71-77.

Shah, S.P., Karaguler, M.E. & Sarigaphuti, M. 1992. Effects of shrinkage-reducing admixtures on restrained shrinkage cracking of concrete, *ACI Materials Journal*, 89(3) May-Jun 1992: 291-295.

Thomas, M.D.A. 1996. Chloride Thresholds in Marine Concrete, *Cement and Concrete Research*, 26 (4): 513-519.

Tuutti, K. 1982. Corrosion of Steel in Concrete, *Swedish Cement and Concrete Research Institute*, Stockholm, Sweden.

Weiss, W. J & Shah, S. P. 1997. Recent trends to reduce shrinkage cracking in concrete pavements, *Proceedings of the Airfield Pavement Conference*, *Aircraft/Pavement Technology: In the Midst of Change*, 217-228.

Zollo, R.F., Ilter, J.A. & Bouchacourt, G.B. 1986. *Proc. RILEM Symposium*, FRC 86 (Ed. Swamy et al.), Vol. 1.